

Crystalline Order and Mechanical Properties of As-Electrospun and Post-treated Bundles of Uniaxially Aligned Polyacrylonitrile Nanofiber

Dorna Esrafilzadeh,² Rouhollah Jalili,¹ Mohammad Morshed²

¹ITA-Co Engineering, Unit 7, No. 63, Sheikh e Bahaii Sq, Tehran, 19949-13434

²Textile Engineering Department, University of Technology, Isfahan, Iran 84154

Received 21 February 2007; accepted 11 October 2007

DOI 10.1002/app.27593

Published online 8 September 2008 in Wiley InterScience (www.interscience.wiley.com).

ABSTRACT: This study investigates the crystalline order and mechanical properties of as-electrospun and posttreated polyacrylonitrile nanofibers. To keep the nanofibers under tension during the posttreatment, a modified method of preparing bundles such as multifilament yarn was used in which the alignment of the nanofibers and linear density of the bundles were controlled successfully. An increase in the nanofibers' diameter from 240 to 500 nm led to the *E* modulus, ultimate strength, and elongation at break of the bundles rising from 836 MPa, 45 MPa, and 38% to 1915 MPa, 98 MPa, and 120%, respectively. The crystallinity index (%) and coherence length of the nanofiber bundles were evaluated through wide-angle X-ray diffraction. The mechanical properties and crystalline order of the nanofiber bundles were both increased

as a result of the posttreatment. Wide-angle X-ray diffraction patterns of annealed bundles showed equatorial diffraction from the (10 $\bar{1}$ 0) reflection at ~ 5.1 Å and from the (11 $\bar{2}$ 0) reflection at ~ 3 Å. The values of the coherence length, crystallinity index (%), ultimate strength, and *E* modulus of the bundles prepared from 240-nm nanofibers increased from negligible, 2%, 1109 MPa, and 48 MPa to 54 Å, 35%, 2235 MPa, and 95 MPa after annealing at 85°C in a mixture of water (95 wt %) and *N,N*-dimethylformamide (5 wt %), respectively. © 2008 Wiley Periodicals, Inc. *J Appl Polym Sci* 110: 3014–3022, 2008

Key words: fibers; nanotechnology; X-ray; electrospinning; PAN

INTRODUCTION

Many applications in textiles and as carbon fiber precursors have been found for polyacrylonitrile (PAN). PAN homopolymer fibers are only rarely used for fiber spinning, and virtually all commercial acrylic fibers are spun from acrylonitrile polymers containing 1–15 wt % comonomers.¹ There are strong intrachain and interchain interactions through secondary bonding because of the large magnitude of the dipole moment of the nitrile groups in PAN fibers. Therefore, upon heating, PAN undergoes a degradation reaction before melting at 320–330°C.^{2,3} The spinning processes most commonly used for acrylic fibers involve highly polar solvents, such as *N,N*-dimethylformamide (DMF), dimethylacetamide, and dimethyl sulfoxide.⁴ Recently, PAN nanofibers have been produced by electrospinning. The electrospinning technique has been recognized as an efficient processing method for manufacturing nanoscale fibrous structures, which are used in many applications such as filtration, reinforcements in composites, and carbon nanofiber precursors.⁵

The majority of textile fibers have a morphology that can be described by the classical two-phase

model. In this model, discrete crystalline domains of the order of several hundred angstroms are mixed with amorphous domains of similar or smaller size. A high degree of crystallinity and high orientation of the crystalline molecular segments impart high tensile strength and modulus to the fibers. The amorphous phase gives rise to flexibility and dyeability.^{6,7}

Whether PAN can be described by the classical model is debatable. In the ordered phase, irregularly twisted yet extended atactic polymer chains are packed hexagonally.⁷ Because of the strong interchain interactions noted previously, this hexagonal columnar phase behaves as a solid, and it is often referred to as a (two-dimensional) crystal.

Wide-angle X-ray scattering of drawn PAN fibers has been shown to have two strong equatorial reflections (Bragg spacings of $d \sim 3.0$ Å and $d \sim 5.3$ Å), indicating an order perpendicular to the fiber axis. This result has frequently been interpreted in terms of hexagonal packing of molecular rods comprising distorted helices or kinked planar zigzags. Some have assumed a single, laterally ordered or paracrystalline phase, whereas others have proposed a two-phase structure with regions of ordered rods and regions of amorphous material or disordered rods.⁷

In the case of nanofibers, their crystalline order may also be of primary importance when these materials are considered for commercial applications.⁸ One characteristic feature of the electrospinning

Correspondence to: R. Jalili (jaliliar@yahoo.com).

ning process is the rapid evaporation of the solvent and the rapid solidification of the polymer material as far as spinning from solutions is concerned. Therefore, structure formation of spun fibers has to happen on a millisecond scale, as is apparent from the high velocity of the whole electrospinning process: fiber deposition rates of the order of several meters per second have been reported.⁹ The nucleation of crystals should, therefore, be strongly retarded, and the structure that results should be far from the equilibrium state. In fact, it has been reported that the crystalline microstructure in electrospun fibers may not be well developed and that the crystal sizes or the long period may be quite small, as observed, for instance, by Reneker et al.¹⁰ They prepared poly(*meta*-phenylene isophthalamide) electrospun nanofibers and found that the as-spun nanofibers had an imperfect crystal structure that could be improved by annealing. To evaluate the crystalline structure of poly(ethylene oxide) (PEO) electrospun nanofibers, Deitzel et al.¹¹ performed wide-angle X-ray diffraction (WAXD) experiments on samples of PEO electrospun nanofibers and PEO powders. The positions of the peak in each diffraction pattern showed that there was no change in the crystal structure induced by the electrospinning process. In fact, the diffraction peaks associated with the PEO nanofibers were significantly broader than the PEO powder diffraction peaks, indicating that the overall crystallinity of the electrospun fibers was poor. Deresch et al.⁸ reported that WAXD of the polyamide-6 electrospun nanofibers did not show a crystalline peak until they were annealed at the elevated temperature of 220°C. To increase the degree of crystallinity and so control the crystal modification, nucleating agents were added to the spinning solution in their experiments. However, nucleating agents were not effective in controlling crystal modification. Zong et al.¹² studied electrospun poly(L-lactic acid) nonwoven membranes by WAXD, but no crystalline peak was observed in their study. In another work,¹³ they carried out a posttreatment on a poly(glycolide-*co*-lactide) membrane to enhance the mechanical and crystalline order of that membrane. Their evaluation indicated that the degree of crystallinity increased by the posttreatment and also by an increase in the treatment temperature from 60 to 90°C. Also, the tensile strength of the annealed membrane under a constant strain of 450% at 90°C for 20 min was 40 MPa, which was 8 times more than that of the untreated membrane. It appears that the retardation of crystallization during the electrospinning of a semicrystalline polymer is universal. The retardation process was attributed to the rapid solidification of the stretched chains at high elongational rates during the later stages of electrospinning, which significantly hindered the formation of crystals. In

other words, the stretched chains did not have enough time to organize themselves into suitable crystal registration before they were solidified.

In addition to the crystallinity, the molecular orientation in polymeric fibers is vital for their performance.⁶ It has been reported that the magnitude of the strain rate in the electrospinning jet is of the order of 10^4 s^{-1} .¹⁴ This elongational flow tends to force the polymeric chains to be oriented in the direction of elongation. Therefore, it is conceivable that this process could give rise to an equally strong elongation of the polymer chains along the fiber axis; this was confirmed by Reneker and Chun⁹ when they studied the electron diffraction patterns of electrospun poly(ethylene terephthalate) fibers. The X-ray diffraction pattern of aligned PAN electrospun nanofibers prepared by Gu et al.¹⁵ showed arcs indicating that molecular chains were oriented within the nanofibers during the electrospinning process. The orientation factor of those nanofibers was 0.127. However, Fennessey and Farris¹⁶ reported that the electrospun PAN nanofibers were unoriented and amorphous when collected onto a stationary target. This was attributed to the rearrangement of the polymer chains and loss of the original molecular orientation after collection. The relaxation of the molecular chain in PAN nanofibers can be restricted if they are kept under tension after being collected.¹⁶

In conventional systems, posttreatment of the PAN bundles is performed by the application of tension to the fibers at temperatures above the glass-transition temperature. After the fibers are extended and subsequently cooled in this stage, if the tension is removed, the fibers will no longer relax. The structure will remain stable until the temperature is raised again to the glass-transition temperature or above.^{17,18} The conditions of posttreatment (i.e., heat treatment) depend on the nature of the polymer and the type of fiber. Heating systems applied in industry include dry air, contact heating elements, water vapor, liquid baths, and so forth.¹⁸

Although there have been many studies on the electrospinning of PAN nanofibers as well as the heat treatments of those nanofibers to make carbon nanofibers,^{19,20} we could find in the literature no detailed study on the crystalline order and mechanical properties of untreated and posttreated electrospun PAN nanofibers; this study investigates the crystalline order and mechanical properties of electrospun PAN nanofiber bundles before and after annealing. The crystallinity of the nanofibers, which were treated under different conditions, was evaluated with WAXD. The posttreatment methods included the annealing of nanofiber bundles in pure water at different temperatures or in a mixture of water and DMF.

EXPERIMENTAL

Materials and preparation

Industrial PAN was received from Iran Polyacryle Co. (Iran) and DMF was obtained from Merck Co. (Germany) as the polymer and solvent, respectively. The weight-average molecular weight and number-average molecular weight of the received PAN were 100,000 and 70,000 g/mol, respectively. The polymer and solvent were dried before use, and 13–17 wt % solutions of PAN in DMF were prepared. Above a concentration of 17 wt %, because of the cohesive nature of the solutions, controlling and maintaining the flow of the polymer solution from the tip of the syringe needle was hard, and so no consistent electrospinning proceeded.

Detailed electrospinning processing conditions were published previously.⁵ In this study, the typical electrospinning parameters were as follows: the applied voltage was 12.5 kV, the distance between the spinneret and the grounded target was 15 cm, and the diameter of syringe needle was 0.7 mm. The flow rate of the polymer solution to the needle tip was maintained so that a pendant drop remained during electrospinning. Solutions were electrospun horizontally onto the target.

Bundles like multifilament uniaxially aligned nanofibers were prepared with a modified method that was previously introduced by the authors.²¹ The bundle preparation parameters were as follows: the width of the gap between two collectors was 3 cm, and the length of the obtained bundles was 2.5 cm, which was approximately 85% of the width of the gap between the two collectors. The linear densities of the bundles were controlled by the adjustment of the time intervals of the electrospinning.

Bundle posttreatment processes

The posttreatments of nanofibers were carried out under two different processes, annealing in hot pure water and annealing in a mixture of hot water and DMF, with the following procedures:

1. The bundles were annealed in hot water at temperatures of 65, 75, and 85°C and in boiling water (ca. 95°C) for 10 min.
2. The bundles were annealed with a mixture of water and DMF at 85°C for 10 min. The solution concentrations were 5, 15, and 25% DMF in distilled water.

To apply tension to the nanofibers during treatment, the bundles were stretched by about 10% of their original length and then were fixed in a special frame. After posttreatments, the bundles were washed and dried at 65°C for 1 h.

Microscopy

The morphology of electrospun PAN nanofibers was studied with a Philips scanning electron microscope (XL-30) (The Netherlands) after gold coating. The average diameter of the electrospun nanofibers was measured by an analysis of scanning electron microscopy (SEM) images with a custom code image analysis program.

Mechanical testing

The mechanical properties of the nanofiber bundles were examined with a Zwick 1446-60 (Germany). The *E* modulus, ultimate strength, and elongation at break were measured. The crosshead speed and the length of the gage were 50 mm/min and 20 mm, respectively. All experiments were carried out at room temperature. The cross-sectional area was calculated from the obtained linear density of the bundles and the density of the PAN fiber from the literature. In each different group, at least 10–30 bundles were examined, and the average of the results was reported.

X-ray diffraction

WAXD patterns of nanofiber bundles were obtained with the Philips X-Pert system using Ni-filtered Cu $K\alpha$ radiation. The diffraction scans were collected at $2\theta = 10\text{--}35^\circ$, and the background was subtracted. The instrumental beam broadening was less than 0.05° . PAN fibers exhibited only two peaks: the primary (10 $\bar{1}$ 0) reflection at $\sim 5.1 \text{ \AA}$ and the weaker, higher order (11 $\bar{2}$ 0) reflection at $\sim 3 \text{ \AA}$, both on the equator. [Note: By convention, four Miller indices (*hkl*) are used for the identification of planes in hexagonal crystals. Index *i* is sometimes omitted because it is equal to $-(h + k)$ by definition.⁶ For two-dimensional structures, such as those formed by PAN, index *l* is equal to zero and may be omitted. Therefore, the planes may be identified with only indices *h* and *k*. The use of these two indices is common only for columnar hexagonal phases and is adopted in this report.]

Through an analysis of the shape and intensity of the primary (10) reflection, the coherence length (L_c) of each nanofiber bundle could be determined. L_c was determined from the analysis of an equatorial scan with the Scherrer equation:⁶

$$L_c = 0.9\lambda / (B \cos \theta) \quad (1)$$

where *B* is the full width (as a function of scattering angle 2θ) at half-maximum of the (10) reflection. This coherence length is often called the crystal size because small crystal size is a major contribution to peak broadening. However, lattice distortions and defects within crystals also contribute to peak broadening. In any case, L_c is a measure of packing perfection.⁶

TABLE I
Experimental Conditions Used To Prepare PAN
Nanofiber Bundles

Concentration (wt %)	Time of electrospinning (s)	Bundle length (mm)	Bundle diameter (μm)
15	—	20	One fiber
15	—	20	Two fibers
14	1	20	3
14	2	25	5
14	3	25	7
14	30	25	500

The calculation of the crystallinity index [CI (%)] was done according to the Dumbleton and Bell method⁴ by the extrapolation of crystalline and amorphous part of the diffraction pattern.

RESULTS AND DISCUSSION

Nanofiber bundle preparation

In order to keep nanofibers under tension during posttreatment, control of the collection process dur-

ing the electrospinning of nanofibers is essential. A series of bundles like multifilament yarns of uniaxially aligned nanofibers were prepared under the experimental conditions listed in Table I. SEM images of the electrospun nanofiber bundles prepared under these conditions are illustrated in Figure 1. As shown in Figure 1, single long nanofibers and bundles with an even diameter of 3 μm were prepared in our laboratory. The bundle thickness and its linear density were affected by the collection period of the nanofiber electrospinning. The longer interval time of electrospinning concluded to collect the denser bundles across the gap between two collectors, so the diameter of the obtained bundles rose with the expansion of the electrospinning time. The length of the collected bundles was approximately 85% of the width of the gap between the collectors. SEM images (e. g. Figs. 1 and 2) show that the bundles were uniform along their length, and this was due to the good alignment of fibers at the deposition stage.

By the extension of the electrospinning time by almost 2 min, thicker bundles, which were more

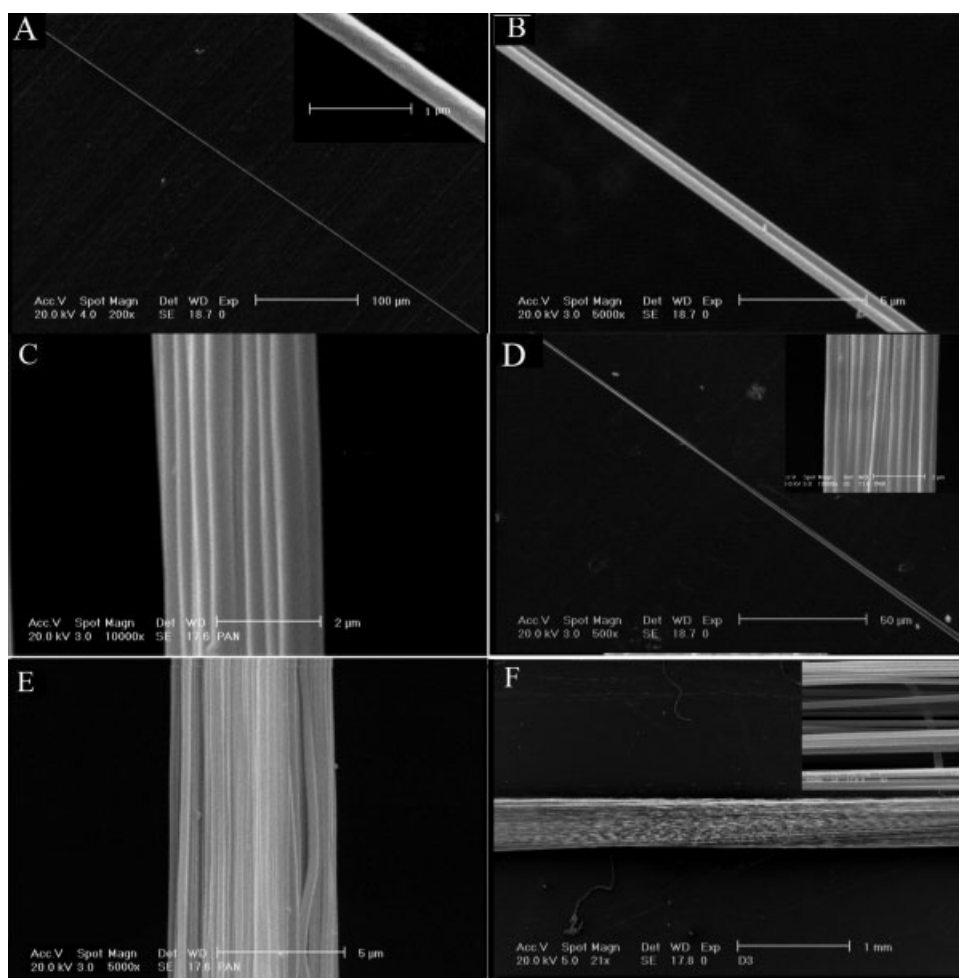


Figure 1 SEM images of (A) a single PAN nanofiber and (B–F) bundles with different widths. The nanofibers diameter was 290 nm.

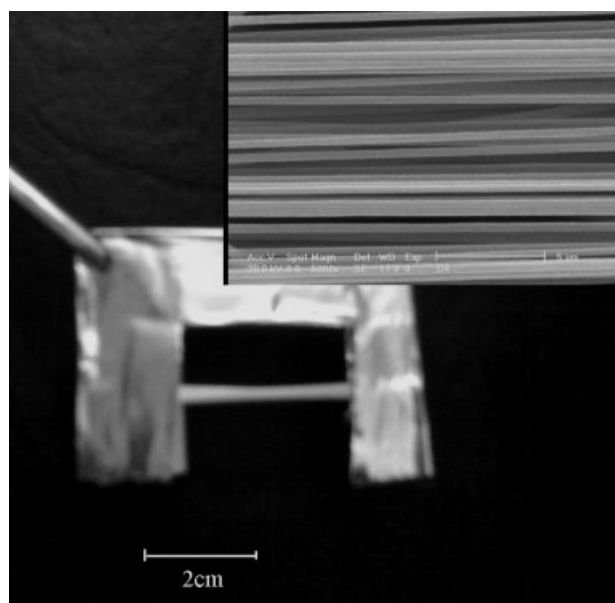


Figure 2 Bundle of nanofibers (time of electrospinning = 120 s; bundle length = 25 mm; nanofiber diameter = 290 nm).

favorable for posttreatment, were produced (Fig. 2). A series of bundles were prepared with different polymer solution concentrations. The experimental conditions are listed in Table II. As the polymer solution concentration increased from 13 to 17 wt %, the nanofiber diameter gradually increased from around 240 to 500 nm. Consequently, the bundles obtained with the same collection time had different linear densities. However, bundles with the same linear density can be prepared from different nanofiber diameters by the adjustment of the time of collection. Table III illustrates experimental conditions under which nanofiber bundles with the same linear density (i.e., 100 g/denier) were produced.

The stress–strain curves of different bundles with the same linear densities are illustrated in Figure 3. The mechanical properties of each bundle are summarized in Table IV. From samples Y1 to Y5, the E modulus, ultimate strength, and elongation at break of the bundles were increased from 836 MPa, 45

TABLE II
Experimental Conditions Used To Prepare PAN Nanofiber Bundles

No.	Concentration (wt %)	Nanofiber diameter (nm)	Linear density of the bundle (g/den)
Y1	13	240	84
Y2	14	290	85
Y3	15	400	108
Y4	16	470	127
Y5	17	500	187

The time of electrospinning was 120 s; the bundle length was 25 mm.

TABLE III
Electrospinning Conditions Giving Nanofiber Bundles with 100 g/den Linear Density

No.	Concentration (wt %)	Nanofiber diameter (nm)	Time of electrospinning (s)
Y1	13	240	140
Y2	14	290	140
Y3	15	400	110
Y4	16	470	95
Y5	17	500	65

The voltage was 12.5 kV; the width of the gap between two collectors was 3 cm.

MPa, and 38% to 1915 MPa, 98 MPa, and 120%, respectively. Bundles produced from thicker nanofibers showed better mechanical properties. However, simultaneous increases in both the strain and stress seem to be unusual. Such a result can be referred to the better alignment of the thicker nanofibers in the bundles. Figure 4 shows SEM images of samples Y1 and Y4. It can be seen that, by an increase in the nanofiber diameter, the alignment of the nanofibers improved significantly. Moreover, there were some entanglements of nanofibers in sample Y1 [Fig. 4(A)].

Figure 5 illustrates the WAXD patterns of samples Y2 and Y5. The bundle with thinner nanofibers exhibited only an amorphous structure, whereas the bundle from the thicker nanofibers exhibited a weak equatorial peak at $2\theta = 16.5^\circ$ corresponding to a spacing of $d \sim 5.3 \text{ \AA}$ from the (10) reflection; although the bundle from thicker nanofibers exhibited some crystallinity of approximately 13%, these findings appear to suggest that crystallization of nanofibers is retarded during electrospinning. With thicker nanofibers (500 nm), the polymer chains probably had more time to organize themselves into crystal structures before solidification. The rise in the E modulus and ultimate strength of bundles with

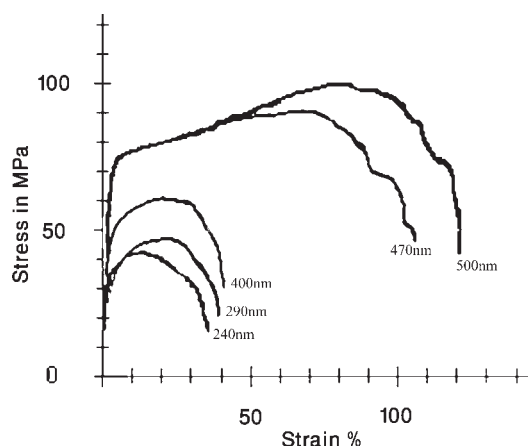


Figure 3 Stress–strain curves of nanofiber bundles. The numbers indicate the nanofiber diameters of the bundles.

TABLE IV
Mechanical Properties of the As-Electrospun Bundles

No.	Nanofiber diameter (nm)	E modulus (MPa)	Ultimate strength (MPa)	Elongation at break (%)
Y1	240	836	45	38
Y2	290	1109	48	39
Y3	400	1187	62	41
Y4	470	1670	93	112
Y5	500	1915	98	120

thicker nanofibers can be tied to the higher crystallinity of the nanofibers and better alignment of them in the bundle, respectively.

Posttreatment of nanofiber bundles

The results of this study showed that the mechanical properties and crystallinity of the as-spun nanofibers were not suitable, especially for the nanofibers with lower diameters. The mechanical properties and crystalline order of most polymeric fibers (e.g., PAN) can be improved by different posttreatments.^{17,18} Because the bundles made from thinner nanofibers

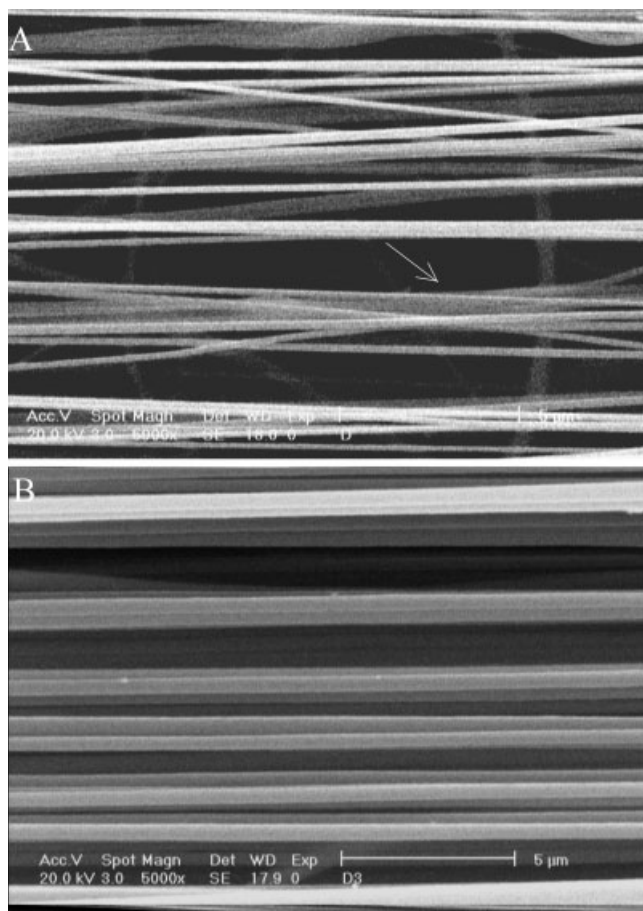


Figure 4 SEM images of (A) sample Y1 (nanofiber diameter = 240 nm) and (B) sample Y4 (nanofiber diameter = 470 nm).

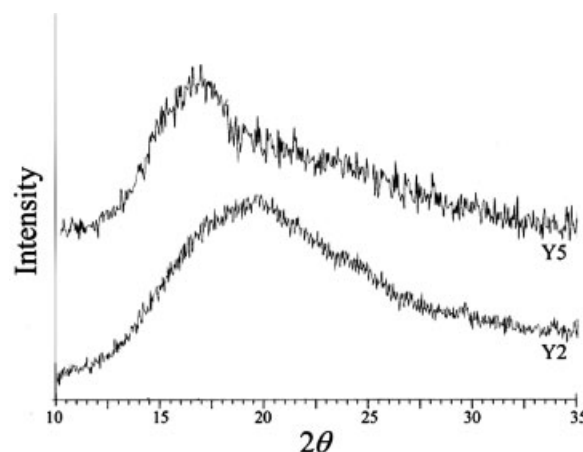


Figure 5 WAXD patterns of electrospun bundles with different nanofiber diameters: sample Y2 (290 nm) and sample Y5 (500 nm).

showed weaker mechanical properties and exhibited a mainly amorphous structure, sample Y2 was subjected to posttreatments to enhance its crystallinity and mechanical properties. It has been reported that the crystallinity of a PAN fiber usually does not

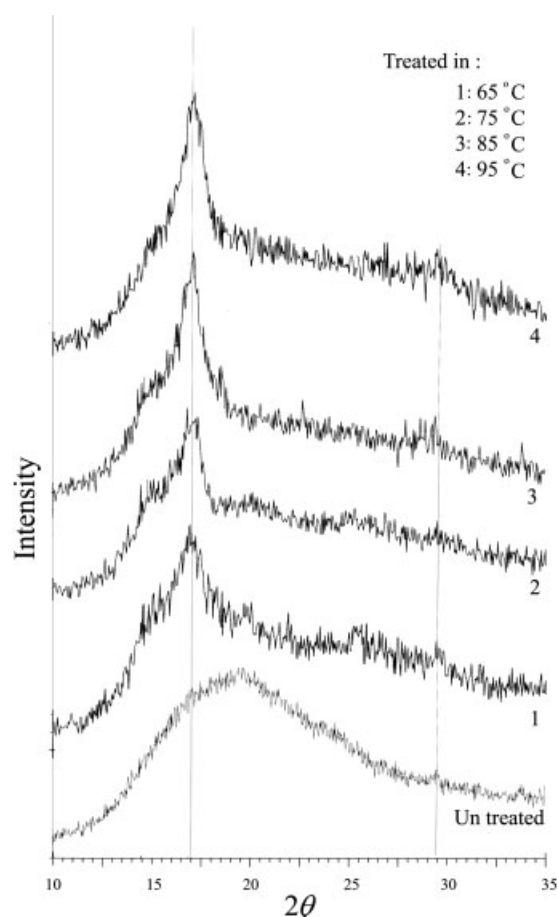


Figure 6 WAXD patterns of Y2 annealed at different temperatures.

TABLE V
Crystalline Properties of As-Electrospun and Annealed Nanofiber Bundles

No.	Annealing temperature (°C)	L_c (Å)	CI (%)
Y2	—	Negligible	2
Y5	—	15	13
Y2-65	65	26	15
Y2-75	75	30	19.6
Y2-85	85	33	21.6
Y2-95	95	35	19.6

improve significantly by stretching,¹⁸ therefore, only 10% elongation before annealing was applied in our experiments.

Annealing in hot water

In a series of experiment, annealing of nanofiber bundles was carried out in hot water at temperatures of 65, 75, 85, and 95°C while the bundles were under tension, and then they were dried. WAXD of annealed bundles exhibits two equatorial diffractions (Fig. 6). The primary reflection (10) has a d -spacing of approximately 5.1 Å, and the weaker (11) reflection is at approximately 3 Å. The ratio of the d -spacing of the two peaks remains $\sqrt{3} : 1$ within experimental accuracy, indicating hexagonal packing.⁶ Two important morphological features can be determined from these equatorial peaks. The first one is the crystal size (L_c), and the other is CI (%), which are presented in Table V. L_c and CI (%) strongly depended on thermal annealing and were improved by post-treatment. The values of L_c and CI (%) increased from negligible and 2% for untreated sample Y2 to 33 Å and 21.6% for sample Y2-85, which was annealed at 85°C. Because the glass-transition temperature of the PAN polymeric fibers in water was in the range of 70°C, in hot water, the molecular mobility appeared to be enough to permit some addi-

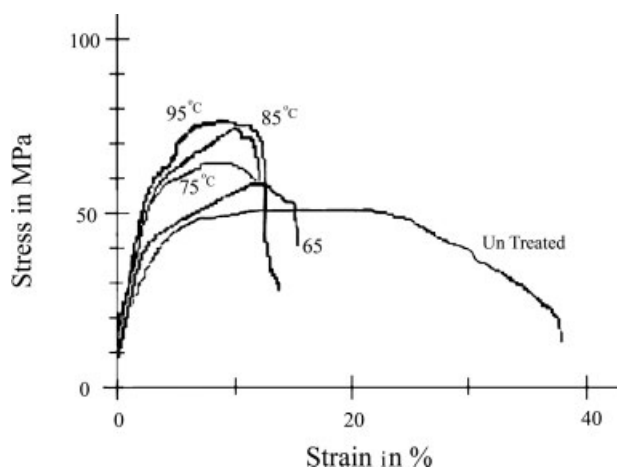


Figure 7 Stress-strain curves of annealed bundles. The temperatures of annealing are indicated.

TABLE VI
Mechanical Properties of the Annealed Bundles

No.	Annealing temperature (°C)	E modulus (MPa)	Ultimate strength (MPa)	Elongation at break (%)
Y2	—	1109	48	39
Y2-65	65	1111	58	17
Y2-75	75	1511	65	12
Y2-85	85	1528	77	13
Y2-95	95	1843	78	13

tional development of the crystalline order; therefore, the polymeric chains had sufficient time to organize themselves into an arranged crystal structure. Bundles annealed in boiling water exhibited lower CI (%) than bundles annealed at 85°C. It seems that molecular motions and mobility were rather high in boiling water, so CI (%) decreased.

The mechanical properties of the as-electrospun PAN nanofiber bundles and the bundles annealed under the aforementioned conditions were compared, and the corresponding stress-strain curves are shown in Figure 7. The mechanical properties of each individual bundle are presented in Table VI. The values of the ultimate strength and E modulus

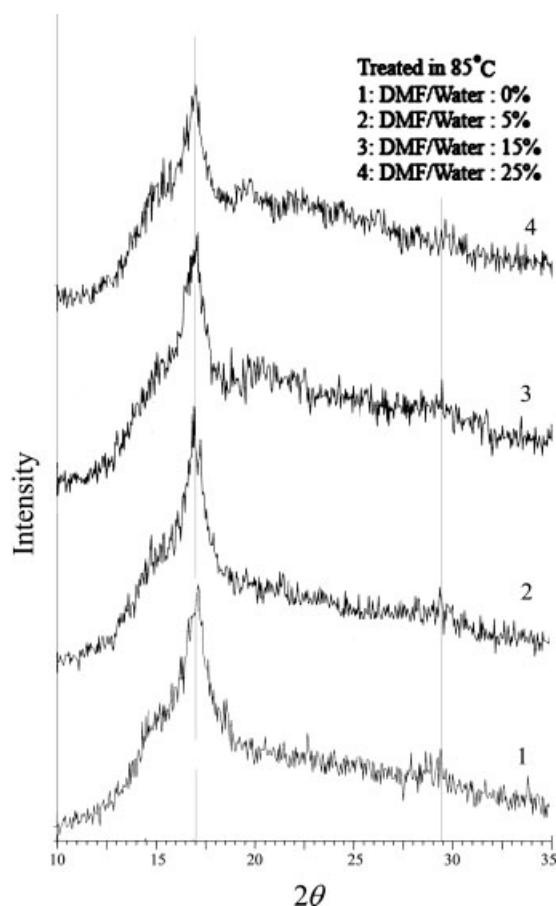


Figure 8 WAXD patterns of sample Y2 annealed at different water/DMF ratios.

TABLE VII
Crystalline Properties of As-Electrospun and Annealed Nanofiber Bundles

No.	DMF/water (wt %)	L_c (Å)	CI (%)
Y2	—	negligible	2
Y2-85	0	33	21.6
Y2-85-5%	5	54	35
Y2-85-15%	15	42	25
Y2-85-25%	25	46	22.5

were both found to increase by 62 and 38% after annealing at 85°C, respectively. The tensile strength did not improve with the annealing temperature rising above 85°C, whereas the E modulus surged by 65% in comparison with that of the as-electrospun bundle. In addition, the elongation at break of the annealed bundles decreased significantly. In other words, the bundles became much stronger with lower elongation after undergoing annealing treatments. This appears to be due to the improvement in the degree of crystallinity, as shown by WAXD studies.

Annealing in hot water with a plasticizer

The crystalline order and mechanical properties of PAN fibers have been improved by postspinning plasticization with DMF.¹⁷ As the annealing in hot water at 85°C exhibited better crystalline order and mechanical properties in our experiments, this annealing temperature was used for posttreatments to enhance the crystalline and mechanical properties of the bundles. The posttreatment conditions with the plasticizer were described earlier. All bundles were first stretched by 10% at room temperature and subsequently annealed and crystallized at 85°C in mixtures of water and DMF with different ratios.

Figure 8 shows the WAXD patterns of the aforementioned treated bundles. The result of L_c and CI (%) of the annealed bundles are shown in Table VII.

The bundle that was annealed in the mixture of water and DMF with 5 wt % DMF showed the best result. The values of L_c and CI (%) increased from negligible and 2% for untreated sample Y2 to 54 Å and 35% for sample Y2-85-5%, respectively. Bundles that were annealed in the hot water with a lower DMF concentration exhibited better crystalline order than those annealed in the pure hot water. By the addition of a small amount of DMF to the annealing bath as a plasticizer, the molecular chains could more easily reorganize themselves into a more appropriate crystalline structure; therefore, L_c and CI (%) were both increased to 54 Å and 35%, respectively. As a reference, the L_c value for a highly oriented acrylic fiber with a diameter of more than 10 μm containing a copolymer of 85% acrylonitrile was 145 Å.⁶ The L_c values obtained in our experiments were for nanofibers containing a copolymer of 90% acrylonitrile and diameters less than 300 nm. To the best of our knowledge, preparing PAN nanofibers with this extent of crystalline order has not been previously reported in the literature. With the concentration of DMF increased to more than 5%, the crystallinity of the nanofibers appeared to decline. Moreover, higher concentrations of DMF showed undesirable effects on the physical structure of the nanofibers. Figure 9 shows SEM images of samples Y-85-5% and Y-85-15%. Nanofibers in sample Y-85-15% were deformed (i.e., they stuck to one another) because of the high concentration of DMF in the annealing bath, whereas those in sample Y-85-5% had a satisfactory structure after annealing.

The mechanical properties of the untreated bundles and the bundles annealed under the aforementioned conditions were compared by their corresponding stress–strain curves, as shown in Figure 10. The mechanical properties of each individual bundle are presented in Table VIII. The values of the ultimate strength and E modulus of the bundles were found to increase by 98 and 101%, respectively,

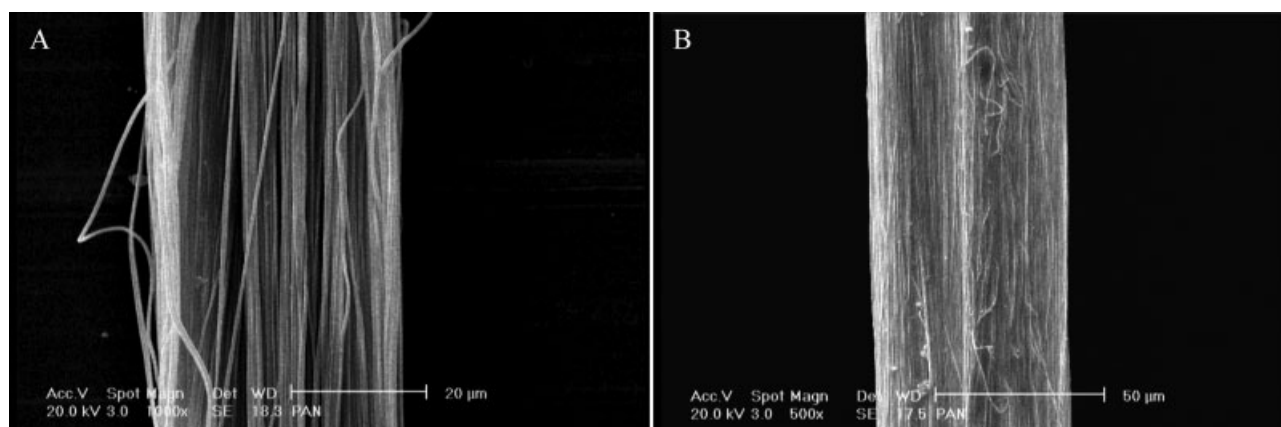


Figure 9 SEM images of annealed bundles in hot DMF/water with DMF concentrations of (A) 5 (sample Y-85-5%) and (B) 15 wt % (sample Y-85-15%).

after annealing at 85°C in the mixture of 95 wt % water and 5 wt % DMF. This could be attributed to the improvement in the nanofiber crystallinity after annealing processes. In addition, when the bundles were annealed in hot DMF/water under tension and dried later, the residual solvent (i.e., DMF) that remained in the core of electrospun nanofibers after electrospinning¹⁶ could be extracted easily; therefore, the rearrangement of the polymer chains and consequent loss of the initial molecular orientation were expected to be limited. The tensile strength and *E* modulus of the bundles declined as the DMF concentration increased to more than 5 wt % in the annealing bath. This could be due to the physical deformation of the nanofibers that appeared in the bundles after annealing under a higher concentration of DMF.

To increase the mechanical properties of the bundles and especially the tensile strength to more than those values obtained in this study, the molecular orientation of the nanofibers should be improved. Work on the effects of poststretching at elevated temperatures on the mechanical properties is currently ongoing.

CONCLUSIONS

Single long nanofibers and ultrathin bundles with a diameter of 3 μm and length of 25 mm from PAN nanofibers were prepared in this research. The thickness and linear density of the bundles were controlled by the control and adjustment of the duration of the nanofiber spinning. There was good alignment of the nanofibers in the as-electrospun bundles. The bundles that were produced from thicker nanofibers had better mechanical properties. WAXD patterns showed that the bundles electrospun from a 17 wt % PAN/DMF solution had a little crystallinity, whereas

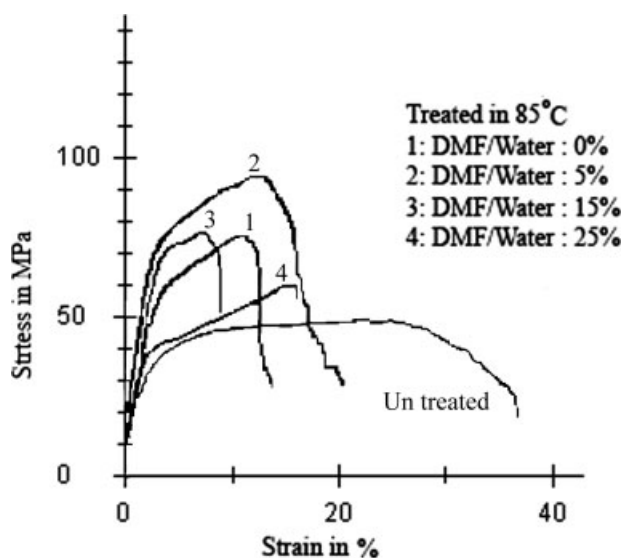


Figure 10 Stress-strain curves of annealed bundles.

TABLE VIII
Mechanical Properties of the Annealed Bundles

No.	DMF/water (wt %)	<i>E</i> modulus (MPa)	Ultimate strength (MPa)	Elongation at break (%)
Y2	—	1109	48	39
Y2-85	0	1528	77	13
Y2-85-5%	5	2235	95	16
Y2-85-15%	15	1824	77	8
Y2-85-25%	25	1475	63	21

the bundles electrospun from 14 wt % PAN/DMF were amorphous.

Both the mechanical properties and crystalline order of the nanofiber bundles were enhanced by annealing in pure hot water or in hot DMF/water. However, annealing in a mixture of hot water and DMF with a small amount of DMF showed better results. The values of the tensile strength, *L_c*, CI (%), and *E* modulus were improved significantly after annealing, although the elongation at break of the annealed bundles decreased distinctly. In other words, the bundles became much stronger with lower elongation after the annealing treatment, and this was attributed to an improvement in the crystallinity after annealing processes.

References

- Sen, K.; Bahrami, S. H.; Bajaj, P. *JMS-REV Macromol Chem Phys* 1996, 36, 1.
- Bahrami, S. H.; Bajaj, P.; Sen, K. *J Appl Polym Sci* 2003, 88, 685.
- Dalton, S.; Heatley, F.; Budd, P. M. *Polymer* 1999, 40, 5531.
- Dumbleton, J. H.; Bell, J. P. *J Appl Polym Sci* 1970, 14, 2402.
- Jalili, R.; Hosseini, S. A.; Morshed, M. *Iran Polym J* 2005, 14, 1074.
- Davidson, J. A.; Jung, H.-T.; Hudson, S. D.; Percec, S. *Polymer* 2000, 41, 3357.
- Masson, J. C. In *Acrylic Fiber Technology and Applications*; Masson, J. C., Ed.; Marcel Dekker: New York, 1995.
- Dersch, R.; Taiqiliu, A. K.; Schaper, A.; Greiner, J. H.; Wendorff, A. *J Polym Sci Part A: Polym Chem* 2003, 41, 545.
- Reneker, D. H.; Chun, I. *Nanotechnology* 1996, 7, 216.
- Reneker, D. H.; Wenxia, L.; Wu, Z. *Polym Prepr Polym Chem* 2000, 41, 1193.
- Deitzel, J. M.; Kleinmeyer, J.; Harris, D.; Tan, N. C. *Polymer* 2001, 42, 261.
- Zong, X. H.; Kim, K. S.; Fang, D. F.; Ran, S. F.; Hsiao, B. S.; Chu, B. *Polymer* 2002, 16, 4403.
- Zong, X.; Ran, S.; Fang, D.; Hsiao, B. S.; Chu, B. *Polymer* 2003, 44, 4959.
- Doshi, J.; Reneker, D. H. *J Electrostat* 1995, 35, 151.
- Gu, S. Y.; Ren, J.; Wu, Q. L. *Synth Met* 2005, 155, 157.
- Fennessey, S. F.; Farris, R. J. *Polymer* 2004, 45, 4217.
- Chen, J. C.; Harrison, I. R. *Carbon* 2002, 40, 25.
- Gupta, V. B. *J Appl Polym Sci* 2002, 83, 586.
- Im, J. S.; Park, S. J.; Lee, Y. S. *J Colloid Interface Sci* 2007, 314, 32.
- Kim, C.; Cho, Y. J.; Yun, W. Y.; Ngoc, B. T. N.; Yang, K. S.; Chang, D. R.; Lee, J. W.; Kojima, M.; Kim, Y. A.; Endo, M. *Solid State Commun* 2007, 142, 20.
- Jalili, R.; Morshed, M.; Hosseini, S. A. *J Appl Polym Sci* 2006, 101, 4350.